

Facile Fabrication of Sandalwood Oil-Based Nanoemulsion to Intensify the Fatty Acid Composition in Burned and Rough Skin

Ved Prakash Giri, Shipra Pandey, Pallavi Shukla, Sateesh Chandra Gupta, Manjoosha Srivastava, Chandana Venkateswara Rao, Shakti Vinay Shukla, Ashish Dwivedi, and Aradhana Mishra*



Cite This: *ACS Omega* 2024, 9, 6305–6315



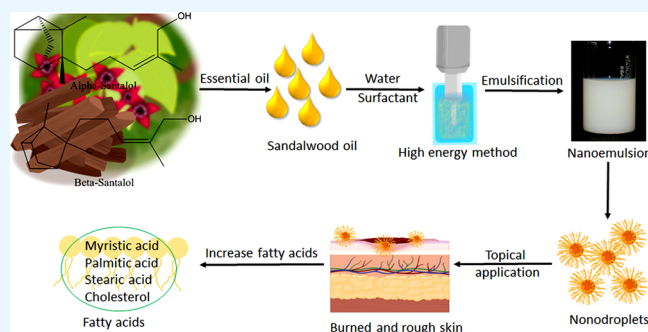
Read Online

ACCESS |

Metrics & More

Article Recommendations

ABSTRACT: The restoration process of burned and rough skin takes a long time and remains a critical challenge. It can be repaired through a combination of proper care, hydration, and topical therapies. In this study, a novel nanoemulsion was synthesized through the high-energy ultrasonication method. A total of five nanoemulsions (NE1–5) were prepared with varying concentrations of sandalwood oil, a nonionic surfactant (poly-sorbate 80), and water. Among them, NE3 had a number of appropriate physicochemical characteristics, such as physiological pH (5.58 ± 0.09), refractive index (~ 1.34), electrical conductivity ($115 \pm 0.23 \text{ mS cm}^{-1}$), and transmittance ($\sim 96.5\%$), which were suitable for skin care applications. The NE3 had a strong surface potential of $-18.5 \pm 0.15 \text{ mV}$ and a hydrodynamic size of $61.99 \pm 0.22 \text{ nm}$ with a polydispersity index of 0.204. The structural integrity and a distinct droplet size range between 50 and 100 nm were confirmed by transmission electron microscopic analysis. The skin regeneration and restoration abilities of synthesized nanoemulsions were examined by conducting an in vivo study on Sprague–Dawley rats. Exposure to NE3 significantly increased the healing process in burned skin as compared to untreated control and nonemulsified sandalwood oil. In another set of experiments, the NE3-treated rough skin became softer, smoother, and less scaly than all other treatments. Enhanced fatty acids, i.e., palmitic acid, stearic acid, and cholesterol, were recorded in NE3-supplemented burned and rough skin compared to the untreated control. The NE3 had outstanding compatibility with key components of skincare products without any stability issues. Its biocompatibility with the cellular system was established by the negligible generation of reactive oxygen species (ROS) and a lack of genotoxicity. Considering these results, NE3 can be used in cosmetic products such as creams, lotions, and serums, allowing industries to achieve improved product formulations and provide better healthcare benefits to humanity.



1. INTRODUCTION

The skin is the largest organ of the human body and consists of three distinct layers that regulate their anatomy and function, namely the epidermis, dermis, and hypodermis. The epidermis is the outer layer of the skin and plays a major role in maintaining the integrity of the stratum corneum (SC).^{1,2} The SC combines with the lipid matrix, which is made up of free fatty acids, ceramides, and cholesterol.^{3,4} The arrangement of these intercellular lipids with regard to the SC cells is crucial for the skin's tightness and maintenance of moisture level.⁵ In order to sustain moisture and permeability, additional lipids are also released in the form of sebum, which is produced by the stratum granulosum and secreted on the upper layer of the skin. Moreover, free fatty acids make the skin's surroundings acidic as well as maintain the skin nourished and protect it from environmental germs.⁶ Sebaceous lipids and epidermal lipids are both part of the lipid barrier of the skin. Particularly, the barrier lipids make up 10% of the SC layer's total mass and

are composed of 50% ceramides, 25% cholesterol, and 15% nonesterified fatty acids.^{4,7,8} Essential fatty acids are a significant part of the lipid layer involved in inflammatory reactions and skin protection. However, burns severely affect the fatty acid composition of the skin. Studies have shown that burns can cause a decrease in the levels of essential fatty acids, such as linoleic and alpha-linolenic acids, in the skin. Linoleic acid makes a major contribution to the formation of the barrier layer and is crucial for the angiogenesis process; hence, widely used in the treatment of blisters and wounds.⁹ In addition, burns discompose the balance between saturated and

Received: May 30, 2023

Revised: December 6, 2023

Accepted: December 28, 2023

Published: January 31, 2024



Table 1. Compositions and Physicochemical Characteristics of the Nanoemulsions (NE1–5)

nanoemulsion	ingredients (V/V)					physicochemical property				
	herbal oil (mL)	nonionic surfactant (mL)	dispersant (mL)	droplet size (nm)	zeta potential (mV)	pH	EC (mS cm ⁻¹)	refractive index	T (%)	phase separation
NE1	0.5/20	1/20	18.5/20	91.29 ± 1.36	-19.9 ± 1.25	5.82 ± 0.07	80.26 ± 0.37	1.34 ± 0.0002	86.2	no
NE2	1/20	0.5/20	18.5/20	229.13 ± 0.18	-15.83 ± 0.45	5.54 ± 0.15	44 ± 0.089	1.34 ± 0.0002	57.9	no
NE3	1/20	1/20	18.0/20	61.99 ± 0.22	-18.50 ± 0.15	5.58 ± 0.09	115 ± 0.23	1.34 ± 0.0002	96.5	no
NE4	1.5/20	0.5/20	18.0/20	179.2 ± 1.57	-12.90 ± 0.79	5.17 ± 0.19	52.26 ± 0.28	1.34 ± NS	90.1	no
NE5	0.5/20	1.5/20	18.0/20	284.8 ± 3.02	-17.40 ± 2.55	5.6 ± 0.07	89.46 ± 0.13	1.34 ± NS	34.6	no

unsaturated fatty acids. Notably, palmitic acid and stearic acid are both important for maintaining the skin's barrier function and overall skin health, while burn injuries can cause a decrease in the levels of palmitic acid and stearic acid in the affected skin.^{10,11}

Numerous studies have mentioned that various essential oils derived from plants can restore deteriorated skin.¹² Sumit et al. prepared a combination of rose and jojoba oil to formulate a beautifying, hydrating, and nourishing oil.¹³ They also formulated a skincare product by mixing lemon, lavender, and wheat germ oil. Similarly, sandalwood oil also has been used for centuries in traditional medicine and skincare practices.¹⁴ Sandalwood oil has a number of beneficial attributes for the skin, including anti-inflammatory, antibacterial, hydrating, astringent, and relaxing properties and can be a valuable addition to the human skincare routine.¹⁵ However, these beneficially attributed oils could not come in common practice because a huge amount of oil is required to make the formulation and direct application. For the past few decades, nanoemulsions have been utilized in the pharmaceutical and cosmetic industries, but skincare products do not contain those bioactive ingredients that balance fatty acids in the lipid layer of burned and rough skin.^{16,17} The cosmetic business focuses on using topical and oral applications of fatty acids and ceramides to make skin smoother and more compact.^{18,19} Many commercial skin protectants contain a variety of nutrients, including fatty acids, carotenoids, ubiquinones, polyphenols, and water- and fat-soluble vitamins, but they fall short of providing the additional nourishment that the skin needs. Therefore, nanoemulsion is an emerging approach to enhance the delivery of bioactive compounds and essential oils in the depth of the skin.²⁰ The nanoscale droplets (1–200 nm) of nanoemulsions enable them for longer stability, better penetration, and targeted delivery.²¹ The oily phase of the nanoemulsions increases the interaction with the lipid layer of the skin, allowing for the effective delivery of the targeted components.²²

This study focused on developing an effective sandalwood oil-based nanoemulsion for balancing the fatty acids in the lipid layer of rough and burned skin. Synthesized nanoemulsions exhibit stable rheological and excellent biocompatible characteristics that enable them to repair damaged skin. It has the potential to close existing gaps in the pharmaceutical and cosmetic sectors.

2. MATERIALS AND METHODS

2.1. General Chemicals and Reagents.

Dulbecco's Modified Eagle's Medium F-12 (DMEM F-12), antibiotic and antimycotic solution, trypsin-EDTA solution (0.25%), L-histidine, 3-(4,5-dimethylthiazolyl-2)-2,5-diphenyl tetrazolium bromide (MTT), and Hank's Balanced Salt Solution (HBSS) were purchased from Sigma-Aldrich (Sigma St. Louis, MO,

USA). Fetal bovine serum (FBS) was purchased from Gibco Life Technologies, USA. Polysorbate 80, hematoxylin, eosin, xylene, chloroform, and paraffin were purchased from HiMedia Laboratories, Mumbai, India. Other chemicals and reagents used were of analytical grade. Sandalwood oil was procured from Shree Krishna Medicose, Rajnandgaon, India.

2.2. Fabrication and Characterization of Sandalwood Oil-Based Nanoemulsions.

2.2.1. Synthesis of Nanoemulsion.

A total of five nanoemulsions, such as NE1, NE2, NE3, NE4, and NE5, were synthesized with a varied range of sandalwood oil and nonionic surfactant (polysorbate 80) by following the method of Pandey et al.²³ Table 1 lists the various constituent concentrations present in the emulsifying mixture. The high-energy probe sonication method was followed for converting the emulsified mixture to nanoemulsion. The mixture was sonicated for 20 min by 10 s on and off cycle at 30% amplitude (Q700 Sonicator, USA).

2.2.2. Physicochemical Characterization.

The physicochemical properties of nanoemulsions were determined by measuring the pH (WTW-inoLab pH 7310, Germany) and electrical conductivity (EC) (HANNA EdgeEC, UK). The refractive index (RI) was analyzed by a refractometer (Leica AR 200, model-57) to determine the isotropic nature of the nanoemulsions. Before the analysis, the sample plate of the refractometer was wiped with acetone, and then, 10 μ L of the nanoemulsion was placed to acquire the RI value. Percent transmittance was measured by a UV-visible spectrophotometer (Evolution 201, USA) to determine the optical properties of nanoemulsions. The stability and phase separation were studied using the centrifugation method; 1 mL of each nanoemulsion was centrifuged at 5000 rpm for 30 min, and phase separation was evaluated by appearance of emulsified solution at 25 ± 2.0 °C. In addition, a pseudo ternary phase diagram was constructed to demonstrate the equilibrium of three different components of nanoemulsion, i.e., water, surfactant, and oil. Hydrodynamic size distribution, polydispersity index (PDI), and zeta potential of nanoemulsions were determined by dynamic light scattering (DLS) analysis (Nano Series Zeta Sizer, Malvern, U.K.) at a fixed scattered angle of 173°. Ten-time diluted samples were used for the DLS analysis. Rheological properties of the nanoemulsions were measured at three different temperatures, i.e., 4, 25, and 45 °C. Viscosity and shear stress were recorded through the Brookfield viscometer V6.SRV, spindle VLA, Middleboro, MA.²⁴ The sample container was filled with 30 mL of nanoemulsion, and spindle rotation was initiated at 60 rpm to acquire rheological parameters.

Based on the physicochemical and mechanical properties of nanoemulsions, NE3 was further characterized by transmission electron microscopy (TEM) analysis (Technai 1321 G2 Spirit TWIN, USA) to determine droplets' definite size and morphology. Briefly, the samples were diluted up to 100

times with deionized water to reduce the effects of repeated scattering. A drop of the diluted sample was kept on a copper mesh grid and dried until proper dehydration. The samples were stained with 2% phosphotungstic acid solution and kept overnight to completely dry. The dried grid was transferred to the system to observe the sample at 100 kV.

2.3. In Vivo Experimental Design. An in vivo study was performed to investigate the impact of NE3 on the re-epithelialization process of burned skin in Sprague–Dawley (SD) rats. Animals were categorized into five groups, i.e., untreated control, positive control (Evion cream, enriched with vitamin E), nonemulsified sandalwood oil (SWO), 1% NE3, and 5% NE3 (where 1 and 5% are the sandalwood oil concentrations in NE3). Six animals were grouped for each treatment and kept in separate cages for 7 days to become familiar with the animal house environment. After that, the dorsal side of the rats was shaved with the help of a hair trimmer for topical application of treatments. The rats were anesthetized with chloroform (99% pure, HPLC grade) inhalation in vacuum desiccators, and a hot rod was touched to their dorsal side for two to five seconds to resemble burned skin in a 15–20 mm area.²⁵ The NE3 and other treatments were applied twice a day on the burned area, while the control group was served without any treatment. The appearance of the burned area was captured by a digital camera for 18 days. During the study, equal amounts of food and water were served to each animal, and their body weight was limited to 150 ± 15 g.

Another set of experiments was performed on SD rats to evaluate the efficacy of NE3 for improving the rough skin. Animals were categorized into four groups, i.e., untreated control, positive control, SWO, and NE3. In this experiment, only 5% NE3 was chosen as the treatment based on its substantial response to burned skin repair. All the treatments were applied on the dorsal side of the shaved area, and changes in rough skin were monitored until 30 days of post-treatment. Both experiments were carried out after the protocol was approved by the Institutional Animal Ethics Committee (IAEC) as per the guidelines of the Committee for the Purpose of Control and Supervision of Experiments on Animals (CPCSEA), New Delhi (Reg. No. 1732/GO/Re/13/CPCSEA). The NIH guidelines were strictly followed for animal handling and care.²⁶

2.4. Extraction of Fatty Acids from Epidermal Skin of Rats. Fatty acid extractions from burned and rough skin tissue of rats were performed using the protocol of Wang et al.²⁷ with some modifications. Briefly, 50 mg of skin tissue was excised and homogenized with a 1× PBS solution in a glass homogenizer (Heidolph DIAX 900). The PBS solution was comprised of 200 ng/mL proteinase K for the degradation of the protein. Homogenized tissue was incubated at 56 °C for 10 min for the lysis of skin layers. The lysate was centrifuged at 12,000 rpm for the removal of residual skin and hair. The supernatant (200 μ L) was mixed with dichloromethane (800 μ L), methanol (400 μ L), and distilled water (200 μ L) for the fatty acid extraction. The mixture was vortexed for one min and centrifuged at 8000 rpm for 10 min. After centrifugation, two layers appeared; the lower layer was transferred into another glass vial and kept at room temperature until the samples became dry. For fatty acid derivatization, the dried sample was mixed with 50 μ L of pyridin and methoxyamine. The sample was mixed properly and kept in a thermomixer for 2 h at 1300 rpm at 37 °C. Thereafter, 50 μ L of 2,2,2-trifluoro-

N-methyl-*N*-trimethylsilylacetamide (MSTFA) was added and shaken again for 30 min at 37 °C at 1300 rpm in a thermomixer.

2.5. Fatty Acid Profiling by GC-MS Analysis. The GC-MS analysis was performed by following the protocols of Bhatia et al.²⁸ Samples were analyzed in a Thermo Trace GC Ultra coupled with Thermo Fisher DSQ II mass spectrometers and provided electron impact ionization at 70 eV to generate mass spectra. Thermo TR50 column (polysiloxane column coated with 50% methyl and 50% phenyl groups) was used for the separation of the lipid contents. Subsequently, a 1 μ L derivatized sample was injected in a column of GC-MS and started with an initial 5 min solvent delay time at 70 °C. The oven temperature was increased up to 330 °C for 5 min; after that, it was again provided 5 min for isocratic, then cooled down to 70 °C, followed by an additional 5 min delay. The helium flow rate was 1 mL, along with a 1/60 split ratio. The GC-MS profile was characterized using REPLIB, WILLY, and NIST mass spectral libraries and matching the chromatogram with appropriate standards. The percent peak area determined the lipid content that has been given on the basis of the peaks detected in the GC-MS chromatogram.

2.6. Histopathology of Excised Tissue. To confirm skin regeneration and restoration after the application of the treatments, a histopathological study was performed. Briefly, 1 mm² of epidermal tissue was dissected and stained with hematoxylin and eosin (H & E) by following the method of Maurya et al.²⁹ The excised tissue was washed with 1× PBS and transferred into a fixing reagent 4% formalin for 24 h. The formalin-fixed tissue was processed through differentially increasing grades of alcohol (70, 80, 90%, and absolute alcohol) and then cleaned with ethanol: xylene (1:1) and pure xylene. The cleaned tissue was embedded in paraffin wax at 65 °C overnight to prepare the blocks and stored at 4 °C until the sectioning. Sections were cut using a semiautomatic microtome (Lyzzer, model no. LT-151-5) and deparaffinized with xylene before being dipped in ethanol at progressively decreasing grades (i.e., 100, 95, and 70%), and then washed with water. Thereafter, H & E staining was done to differentiate the structural state of the tissue. Hematoxylin stains the acidic region of the cytoplasm, cartilaginous matrix, and nucleus of cells in blue, whereas eosin stains the basic regions and collagen fibers in pink color.³⁰

2.7. Compatibility of NE3 with Key Ingredients of Conventional Skincare Products. The NE3 was amended with key constituents of skincare products, which are typically used in the cosmetic industries. Thus, the sandalwood oil-based nanoemulsion (NE3) was formulated as a “nanoserum” that comprised 75 μ L/mL NE3, 15% glycerol, and 200 mg/mL herbal gel. Usually, glycerol and aloe vera gel are used in skin serums as key ingredients which provide thickness in the formulation, give longer time adhesion, and make the product easy to use.

2.7.1. In Vitro Biocompatibility Assessment. After the successful development of NE3-based nanoserum, two comparative in vitro studies were carried out to evaluate the cellular toxicity and biofriendly response. The NE3-supplemented herbal nanoserum was compared to a commercial skin serum (i.e., herbals white glow intensive skin serum and moisturizer, Lotus Botanicals LLP, Visakhapatnam, India), which had comparable traits. Notably, measuring the level of reactive oxygen species (ROS) and DNA damage in cells or tissues is an important way to assess the safety and efficacy of

compounds. Various methods can be used to measure ROS levels and DNA damage, such as fluorescence assays and DNA fragmentation assays. In the present study, 2',7'-dichlorofluorescein-diacetate (DCF-DA) assay and comet assay were performed on human keratinocyte (HaCaT) cells to demonstrate the degree of ROS level and DNA damage state after exposure to nanoserum.

DCF-DA assay: DCF-DA labeling was performed to detect ROS levels in nanoserum-exposed HaCaT cells. Two distinct concentrations (i.e., 0.25 and 0.50%) of herbal nanoserum and commercial serum were used to treat the cells for 24 h in dark conditions. The control cells were served without any treatment. After that, cells were incubated with 10 μM of carboxy-DCFH₂-DA in HBSS for 30 min at 37 °C in dark conditions, and fluorescence scattering emission was observed under a fluorescence microscope (FLoid Cell Imaging Station, Life Technologies, CA).³¹

Comet assay: alkaline single-cell gel electrophoresis was performed to detect single-stranded DNA lesions. HaCaT cells were grown in 12 well plates until 50% confluence, and NE3-based nanoserum and commercial serum were applied on the monolayer of the cells while untreated cells served as control. After overnight incubation, cells were harvested and resuspended in chilled PBS. Approximately, 20 μL of cell suspension ($\sim 10^4/\text{mL}$ cells) was mixed with 80 μL of 0.5% low melting agarose (LMA) and layered on precoated slides with 200 μL normal agarose (1%). A third layer of 1% LMA was laid down on slides and left for 10 min to solidify. The slides were kept at 4 °C in a lysing solution (100 mM Na₂EDTA, 2.5 M NaCl, 10 mM Tris pH 10 with 1% Triton X-100) for 1 h. Fresh ice-cold alkaline electrophoresis buffer (1 mM Na₂EDTA, 300 mM NaOH, and 0.2% DMSO, pH 13.5) was poured into the chamber of the horizontal gel electrophoresis unit, and slides were left for 20 min to unwind the DNA before electrophoresis at 22 V (0.8 V/cm) and 300 mA current for 30 min. To neutralize the alkali, the slides were washed with tris buffer (0.4 M, pH 7.5) and stained with 100 μL ethidium bromide (20 g/mL). Following that, cells were scored using an image analysis system (Komet-5.0; Kinetic Imaging, Liverpool, UK) and linked to a fluorescent microscope (DMLB, Leica, Germany). Each slide had about 50 cells examined. The DNA lesion in the cells was calculated as a percentage of the head DNA, tail DNA, and olive tail moment (OTM).³²

2.8. Statistical Analysis. In vitro experiments were carried out at least three times, while six replicates were included in in vivo studies. Mean values are shown with standard errors (SE) in the graphs or tables. ANOVA: a single factor was used to evaluate the significance level of three/six technical replicates ($p \leq 0.05$) between the treatments.

3. RESULTS AND DISCUSSION

3.1. Physicochemical Characteristics of Nanoemulsion. A total of five nanoemulsions (NE1–5) have been synthesized with various concentrations of sandalwood oil and surfactant. The concentrations of ingredients and physicochemical characteristics, including droplet size, zeta potential, pH, EC, RI, and % transmittance, are shown in Table 1. Notably, the slightly acidic pH of nanoemulsions is an important factor for increasing skin hydration as well as scaling up their effectiveness.³³ In the present study, synthesized nanoemulsions (NE1–5) exhibit an acidic pH range between 4.0 and 6.0 (Table 1), where NE3 had a pH of

5.58 ± 0.09 with high electrical conductivity ($115 \pm 0.23 \text{ mS cm}^{-1}$), which is obvious for outstanding compatibility to the physiological state of the skin. It can retain skin hydration and prevent microbial growth, which could eventually encourage the regeneration of damaged tissues.^{34,35} According to Ribeiro et al., the pH of nanoemulsions used in cosmetic products should be in the range of 4 to 6, which can help to maintain the skin's barrier function and reduce the risk of skin irritation and sensitivity.³⁶ Additionally, the RI is a salient feature of cosmetic products. The isotropic nature and transparency of the emulsions depend on their RI. The isotropic property of the liquid solution determines its uniformity in all directions and gives a glossy effect to the applied area of the skin. The NE1–5 had a 1.34 RI which is almost equal to the water (i.e., 1.3–1.4) (Table 1). Shah et al. stated that the RI of a homogeneous nanoemulsion should be in the range of 1.0 and 2.0 RI.³⁷ The 1.3 RI value of NE1–5 indicates an important property that would be suitable for use in skincare products. However, turbidity is another unique characteristic of nanoemulsions for cosmetic products. In the present study, turbidity was measured in terms of percent light transmittance ($T\%$).

Among NE1–5, the highest percent transmittance (96.5%) was observed in NE3 as compared to all others (Table 1). No phase separation was observed in the centrifugation process, which advocated the uniform distribution, longer stability, and excellent homogeneous properties of the nanoemulsions.

In addition, viscosity is the principal parameter for optimizing the flow of fluids at a particular temperature and shear stress. In the present study, NE1–5 had a dynamic viscosity from 0.75 to 2.5 cP at 4 to 45 °C. Maximum viscosity and shear stress were recorded in NE3 at 4 and 45 °C, (Figure 1), which address the contemporary need of the cosmetic

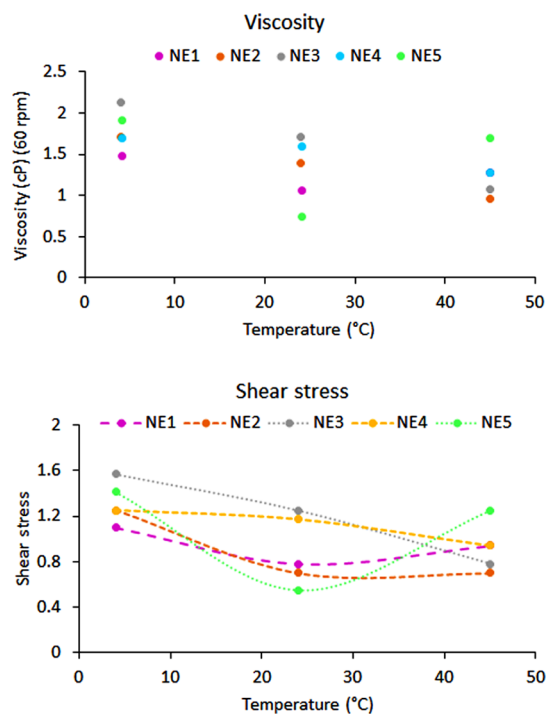


Figure 1. Rheological behavior of nanoemulsions (NE1–5). A dynamic viscosity and shear stress at a wide range of temperatures (i.e., 4, 25, and 45 °C).

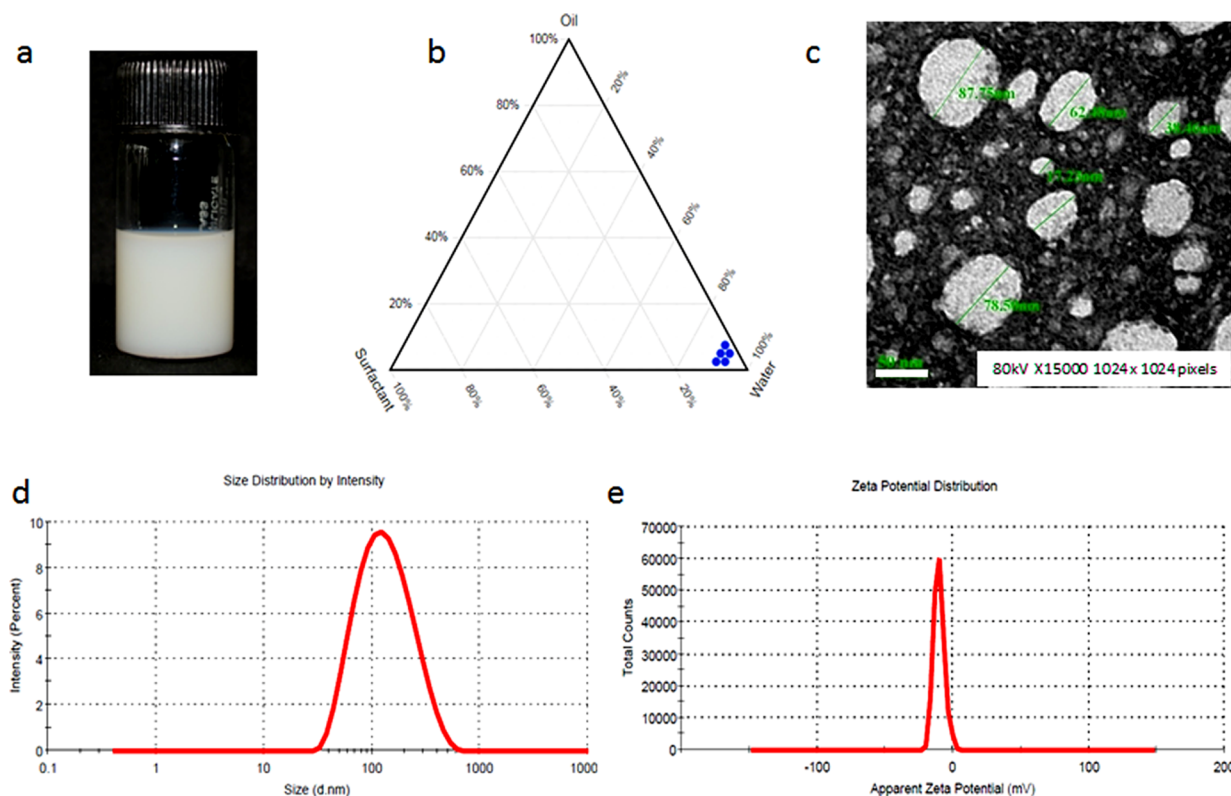


Figure 2. Synthesis and characterization of sandalwood oil nanoemulsion: (a) visual appearance of NE3, (b) ternary phase diagram of NE3, (c) TEM micrograph, scale bar 50 nm, (d) hydrodynamic size of NE3, and (e) surface zeta potential of NE3.

industries. The NE3 nearly fulfills the challenging measures of a skincare product with its physicochemical characteristics and rheological behavior. Generally, nanoemulsions used in skin care products have low to medium viscosity, which allows them to spread easily and be absorbed into the skin without leaving a heavy or greasy residue.

Among all five nanoemulsions (NE1–5), NE3 exhibits excellent characteristics of standard nanoemulsion which appeared homogeneous and whitish in color. The ternary phase diagram demonstrates varying component concentrations as well as delineates a monophasic area (Figure 2a,b). Particularly, a ternary phase diagram shows the behavior of a three-component system under various conditions including temperature and pressure. TEM analysis ensured the structural appearance and a definite droplet size range between 50 and 100 nm (Figure 2c). The NE3 had a dynamic size range of droplets in a spheroid or quite irregular shape, which yielded a stable herbal nanoemulsion. Its hydrodynamic droplet size distribution ranges up to 61.99 ± 0.22 nm with a lower PDI (0.204 ± 0.001) (Figure 2d). The longer stability and greater diffusibility of bioactive components to the targeted region can be aided by the smaller droplet size of the nanoemulsions, where a lower PDI value ensures the homogeneity of the emulsified mixture. Additionally, NE3 had an abundance of negative surface potential up to -18.50 ± 0.15 mV (Figure 2e) which is enough to create an energy barrier between nanosized droplets because a vigorous surface potential possibly suppresses the sedimentation, flocculation, and agglomeration possibilities.³⁸

3.2. Burned and Rough Skin Improvement. Wound healing is a systemic process and can be categorized into four phases, such as hemostasis, inflammation, proliferation, and

maturation. Particularly, the burned skin regeneration process depends on numerous factors, including the types of burn injuries, the severity and size of the wound, the patient's health, and the materials used to cover the burned area.³⁹ In the present study, an in vivo investigation was carried out using NE3 and three other treatments i.e., untreated control, a commercially available cream (Evion cream, enriched with vitamin E), and SWO, to assess how SD rat' burned tissue recovered over the course of 18 days (Figure 3A). Surprisingly, a significantly higher skin regeneration rate was observed with NE3, resulting in a smaller wound area of 8.89 ± 0.73 and 6.35 ± 0.73 mm ($p < 0.05$) on days 13 and 18, respectively. Whereas, a lower regeneration rate was recorded with the untreated control, positive control, and SWO, which appeared significantly larger burned wound area by 20.32 ± 0.00 , 16.51 ± 0.73 , and 13.97 ± 0.72 mm, respectively, as compared to NE3-treated wound ($p < 0.05$) (Figure 3B). However, on day 18, a different pattern was observed with the untreated control, positive control, and SWO by 10.16 ± 0.00 , 7.62 ± 0.00 , and 12.7 ± 1.46 mm, respectively. The tissue regeneration with NE3 was visually apparent from day 13, and complete restoration was found on day 18, while NE1 did not show a noticeable enhancement in the healing process relative to all other treatments.

In another set of experiments, the NE3 was applied on the rough skin of SD rats along with the positive control, SWO, and untreated control. After regular application of all the treatments on the rat skin for up to 30 days, NE3-treated skin appears softer, smoother, and less scaly than all other treatments (Figure 4).

There is some scientific evidence suggesting that sandalwood oil has skin repair properties and that its nanoemulsion

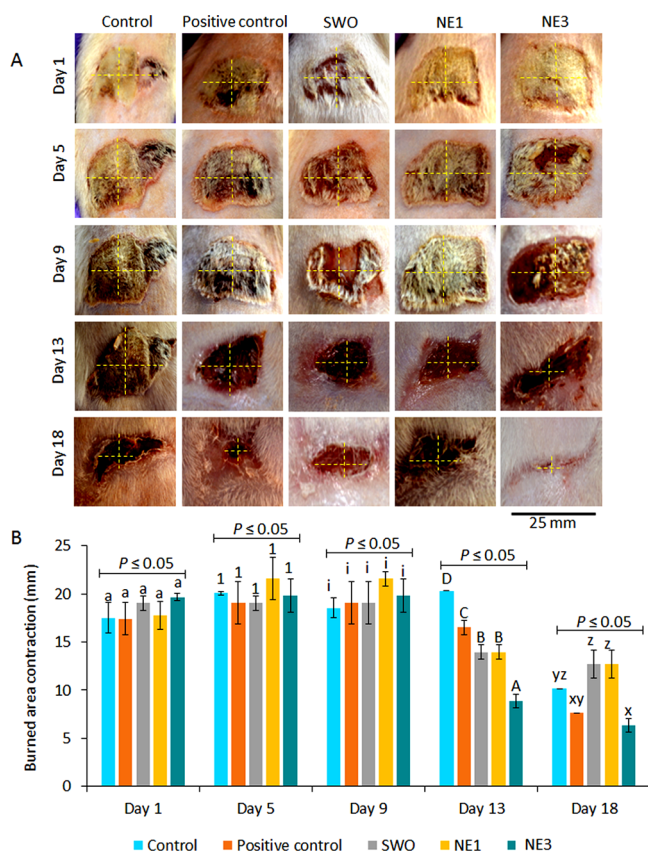


Figure 3. In vivo evaluation of burn wound healing process at different time intervals: (A) visual appearance of wounds after exposure to different treatments *viz*; untreated control, positive control, sandalwood oil (SWO), and nanoemulsion (NE1 & NE3), (B) measurement of burned wound area at a different time interval. The means of six replicates sharing different letters/numbers differ significantly from each other at $p \leq 0.05$.

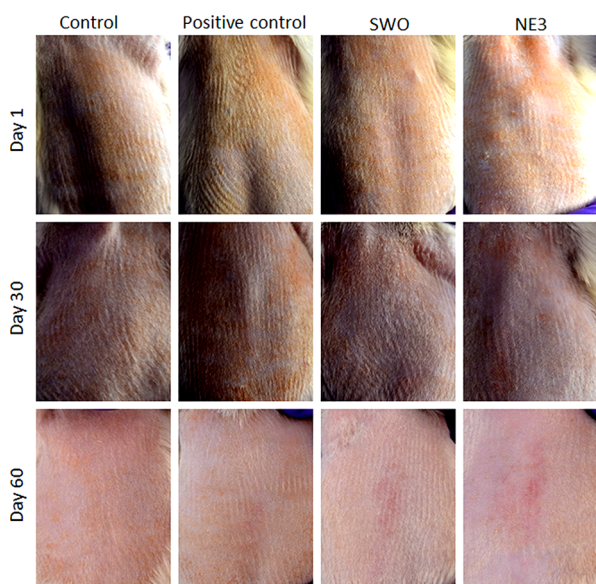


Figure 4. Observation of changes in rough skin after exposure to different treatments *viz*; untreated control, positive control (commercial skin toner), sandalwood oil (SWO), and nanoemulsion (NE3) at 30 and 60 days.

can improve the delivery and efficacy of active ingredients in skincare products.^{40,41} Anand et al. described that sandalwood oil has anti-inflammatory and antioxidant properties that may help promote wound healing and reduce scar formation.⁴² They suggested that a nanoemulsion of sandalwood oil could improve the stability and penetration of the oil into the skin. In the present study, it is well corroborated that the smaller droplet (≈ 61 nm) size of NE3 could improve the penetration of sandalwood oil active ingredients into the skin and promote restoration of burned and rough skin. This is because smaller droplets have a larger surface area, which increases contact with the skin and allows for a more effective absorption.

3.3. Fatty Acid Profile of Burned and Rough Skin.

Fatty acids are essential components of the skin and play important roles in maintaining skin health and function. The fatty acids help to form the skin barrier, which prevents water loss and protects the skin from environmental stresses. Particularly, palmitic acid is the most abundant fatty acid in the skin, making up about 20–25% of the total fatty acids present in the SC. Other important fatty acids also found in the skin include linoleic, oleic, and stearic acid. Linoleic acid is an essential fatty acid that cannot be produced by the body and must be obtained through a diet or external supplements. In the present investigation, palmitic acid, stearic acid, and cholesterol were higher (i.e., 28.24 ± 2.14 , 31.83 ± 2.95 , and $14.24 \pm 1.10\%$, respectively) in NE3-treated burned skin tissue. However, a comparatively lower degree of these fatty acids was recorded in all other treatments, including a positive control, SWO, and untreated control (Table 2). Fatty acid enhancement in NE3-treated burned skin indicated the significant role of nanoemulsion in maintaining moisture, hydration, and nourishing the skin because it carried bioactive compounds of sandalwood oil that can strengthen the skin's lipid barrier.

In addition, an excellent state of palmitic acid and stearic acid was recorded in the NE3-supplemented rough skin tissue of SD rats. After 30 days of exposure, a higher proportion of palmitic acid and stearic acid (i.e., 17.89 ± 1.54 and $18.81 \pm 1.89\%$, respectively) was evident in NE3-treated skin; however, positive control and SWO also had proportional increases in these important fatty acids as compared to untreated control (Table 2). It has been reported that palmitic acid and stearic acid are good emollients for the skin and are more abundant in younger people than in older ones.⁴³

There is limited research available on the effects of sandalwood oil on the fatty acid composition of the skin, some studies suggest that the active compounds in sandalwood oil may have a positive effect on the skin's lipid barrier.^{14,15} In a study, the topical application of alpha-santalol was found to increase the level of ceramides, cholesterol, and fatty acids in the SC.⁴⁴ According to this study, sandalwood oil may improve the lipid barrier of the skin by boosting the skin's fatty acid content. However, it is important to mention that more insightful research on lipidomic analysis is needed to fully understand the effects of sandalwood oil on the skin and its fatty acid composition.

3.4. Histopathology of Burned and Rough Skin. After the promising appearance of extensive wound contraction with NE3 exposure, a microscopic observation was performed to demonstrate the structural state of the sebaceous glands and the repair process. Importantly, NE3-treated skin tissue clearly shows increased density and reformation degree of sebaceous glands in comparison to all other treatments (Figure 5). The

Table 2. Fatty Acid Profile of Burned and Rough Skin through GC-MS Analysis

GC-MS profile of burned skin						
retention time	compounds	formula	relative area percent			
			control	positive control	SWO	NE3
8.04	1-(3-methylbutyl)-tetramethylbenzene	C15H24				
11.21	glycerol	C12H32O3Si3				1.27 ± 0.21
16.27	1H-indole-3-acetonitrile	C13H16N2Si			5.81 ± 0.49	3.19 ± 0.29
20.35	1,3-benzoxazol-2-amine	C13H22N2OSi2			1.15 ± 0.12	0.73 ± 0.01
26.81	myristic acid	C17H36O2Si				1.86 ± 0.12
30.6	palmitic acid	C19H40O2Si	5.42 ± 0.42	12.07 ± 1.32	16.70 ± 1.36	28.24 ± 2.14
34.05	stearic acid	C21H44O2Si	5.75 ± 0.42	11.20 ± 1.54	12.92 ± 1.15	31.83 ± 2.95
34.27	linoleic acid	C21H40O2Si	0.54 ± 0.02			0.35 ± 0.01
35.98	tert-nonyl mercaptan	C9H20S	0.84 ± 0.04			
37.55	1,3-di-stearin	C39H76O5	1.26 ± 0.12			
39.12	tetratetracontane	C44H90	1.38 ± 0.16			
40.61	tritetracontane	C43H88	1.31 ± 0.09			
42.03	cholest-7-en-6-one, 3-(acetyloxy)-9-hydroxy	C29H46O4	1.13 ± 0.13			
48.05	cholesterol	C30H54OSi	10.22 ± 1.01	8.37 ± 0.75	12.46 ± 1.33	14.24 ± 1.10
49.76	stigmasterol	C32H56OSi	30.25 ± 3.5	8.66 ± 0.69		
GC-MS profile of rough skin						
			control	positive control	SWO	NE3
11.21	glycerol	C12H32O3Si3	1.93 ± 0.12	2.36 ± 0.19	1.07 ± 0.14	3.51 ± 0.29
16.27	1H-indole-3-acetonitrile	C13H16N2Si	1.6 ± 0.17	4.02 ± 0.39	2.14 ± 0.19	1.12 ± 0.14
20.35	1,3-benzoxazol-2-amine	C13H22N2OSi2		1.63 ± 0.11	0.9 ± 0.02	0.19 ± 0.01
26.79	myristic acid	C17H36O2Si				1.48 ± 0.12
29.58	butyl 11-eicosenoate	C24H46O2	0.21 ± 0.01			0.26 ± 0.02
30.6	palmitic acid	C19H40O2Si	8.61 ± 0.75	18.34 ± 1.45	21.26 ± 2.14	17.89 ± 1.54
34.08	stearic acid	C21H44O2Si		9.85 ± 0.86	30.04 ± 2.25	18.81 ± 1.89
34.27	linoleic acid	C21H40O2Si			2.74 ± 0.21	0.32 ± 0.02
42.26	diisooctyl phthalate	C24H38O4			1.83 ± 0.15	
48.07	cholesterol	C30H54OSi		0.73 ± 0.01	19.57 ± 1.78	0.32 ± 0.01

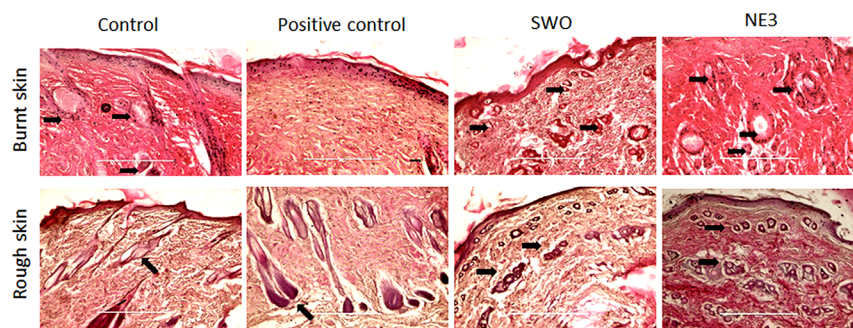


Figure 5. Histopathology of cutaneous tissues of burned and rough skin with H & E staining. The black arrows indicate the cross-section of sebaceous glands and their structural state.

sebaceous gland helps in secreting the sebum on epidermal tissue, which makes skin moist and also prevents microbial attack.⁴⁵ The higher density of sebaceous glands confirmed that NE3 promoted a tissue regeneration process in burned skin and showed similar organization to the native state. However, the restoration of skin structures was noticeably less pronounced in all other treatments.

In addition, the histopathology of rough skin clearly evidenced well organized and structured sebaceous glands in NE3-treated skin as compared to all other groups (Figure 5). Generally, sebaceous glands release sebum onto the SC to keep the skin moist, taut, and sterile.⁴⁶ Interestingly, NE3 exhibits the ability to both accelerate the healing process and continually remodel the tissue, resulting in a healthy skin shape.

There is some evidence to suggest that nanoemulsions can help restore the structural and functional properties of the sebaceous gland in the skin.^{12,47} The sebaceous glands produce sebum, which is a mixture of lipids and other substances that helps moisturize and protect the skin. When the sebaceous gland becomes dysfunctional, it can lead to skin problems, such as acne and dry skin. Ghose et al. described the nanocarrier-based therapies that are able to restore the activity of the sebaceous gland.⁴⁸ Many other researchers observed an increase in sebum production and an improvement in the structure of the sebaceous gland after the topical applications of nanocosmeceuticals.^{49,50}

3.5. NE3 More Compatible with Key Constituents of Traditional Skincare Products. The aforementioned findings evidenced that NE3 had a great potential to balance

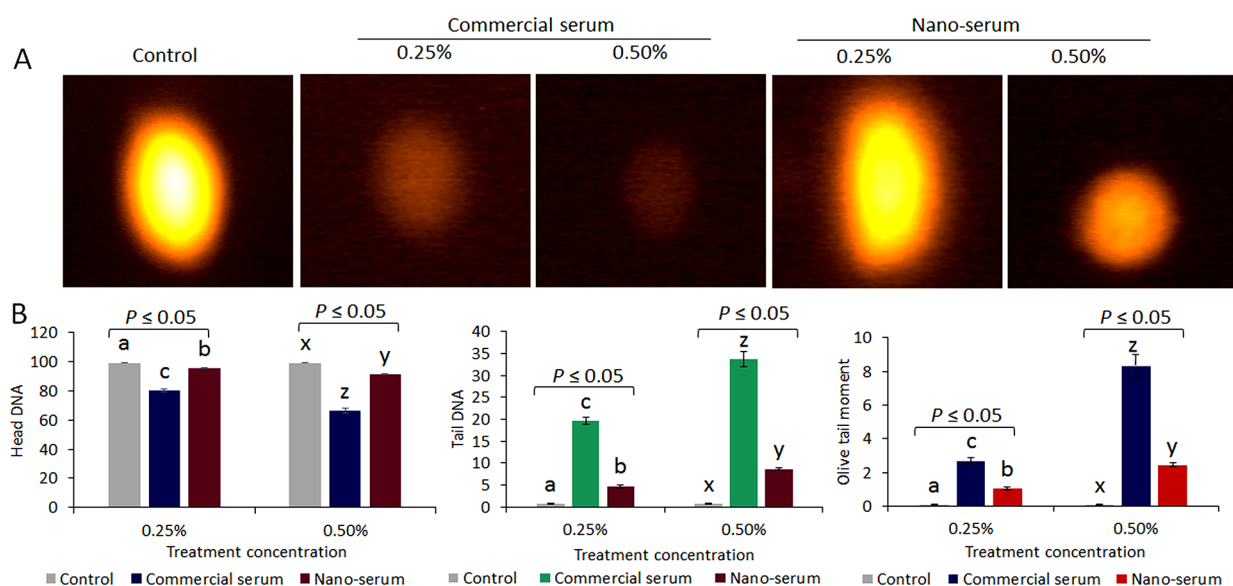


Figure 6. Comet assay: (A) qualitative evaluation of genotoxicity in HaCaT cells after the exposure of commercial serum and herbal nanoserum. (B) Quantitative determination of head DNA, tail DNA, and olive tail moment. The means of three replicates sharing different letters differ significantly from each other at $p \leq 0.05$.

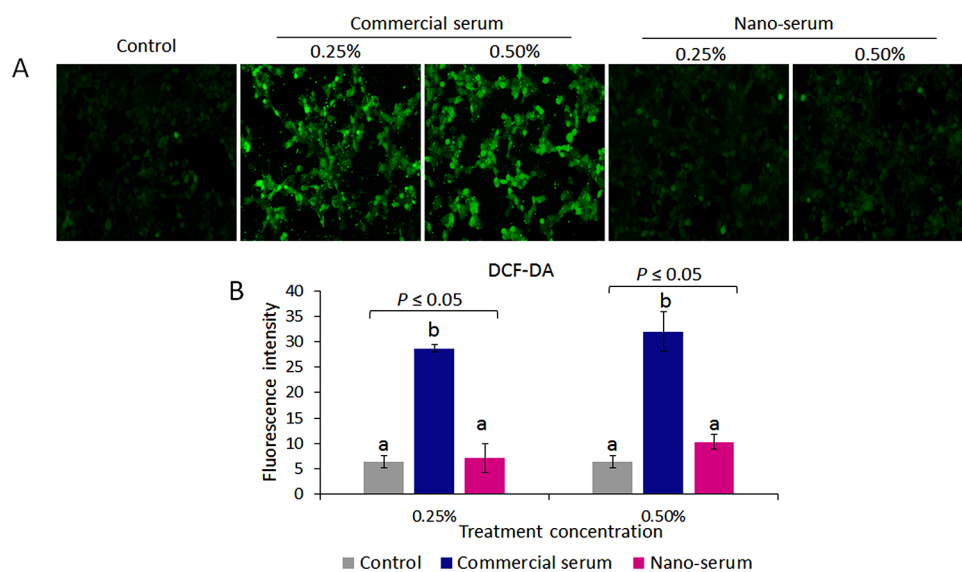


Figure 7. DCF-DA assay. (A) Fluorescence microscopic observation of ROS level in commercial serum and nanoserum-treated HaCaT cells. (B) Quantification of fluorescence intensity (by ImageJ software) of cells after exposure of commercial serum and nanoserum. The means of three replicates sharing different letters differ significantly from each other at $p \leq 0.05$.

the fatty acids in burned and rough skin and to provide a structural state of sebaceous glands. The NE3 is made up of similar basic constituents of conventional skincare products (e.g., oil, water, and surfactants). Therefore, it is more compatible and well incorporated with the key affinities of existing formulations without causing stability issues or other problems. Researchers mentioned that the technological use of nanoemulsions is a promising advancement in the transdermal delivery of active substances. Because it has distinctive characteristics such as nanosized droplets (≤ 100 nm), large interfacial area, transparent appearance, and great solubilization capacity with low viscosity.^{51,52}

In order to evaluate the compatibility of NE3-comprised nanoserum to human cells, a comet assay has been performed on the HaCaT cell line to examine the DNA damage involving

single-strand breaks. Due to its sensitivity and reliability, it is widely used for detecting single-stranded DNA damage in single cells. In electrophoresis conditions, the migration of negatively-charged broken and fragmented DNA moves away from the nucleus and toward the anode. The rate of DNA migration is proportional to the extent of DNA damage. Damaged DNA has a prominent comet-like tail, whereas undamaged DNA has a bright head and an intact nucleus.⁵³ In this investigation, the cells treated with the commercial serum (0.25 and 0.50%) showed a significant increase in the percentage of the olive tail moment and tail DNA both qualitatively (Figure 6A) and quantitatively (Figure 6B) under dark conditions, compared to the cells treated with the herbal nanoserum and the untreated cells. Herbal nanoserum-treated cells (0.25 and 0.50%) resulted in a lower percentage of tail

DNA and olive tail moment, indicating the excellent cellular compatibility and nongenotoxic behavior of NE3-comprised nanoserum.

In addition, many studies demonstrated that oxidative stress is indeed responsible for the generation of the large-scale deletion of the mitochondrial DNA, thereby inducing cutaneous aging. Decreasing ROS formation is thus a promising strategy to prevent and minimize skin damage. The study of photostable molecules derived from natural products for the development of lotions is gaining popularity. However, the synergistic effects of secondary metabolites in plants allow for the acquisition of multiple biological effects from a single product.⁵⁴ In the present study, the role of oxidative stress in the generation of intracellular ROS was investigated in the HaCaT cell line. Higher ROS levels appeared in cells treated with commercial serum (0.25 and 0.50%) through elevated green fluorescence as compared to cells treated with herbal nanoserum (0.25 and 0.50%) and untreated control cells. The state of ROS level in cells treated with herbal nanoserum was comparable to untreated control cells (Figure 7A,B). Nonconsiderable degree of ROS in herbal nanoserum-treated cells indicates its nonoxidative nature that can prevent cellular damages. In a similar way, Jerobin et al. studied the genotoxicity and induction of ROS in human lymphocyte cells after exposure to neem nanoemulsion and recorded a nonconsiderable proportion of tail DNA and a negligible state of ROS at <1.2 mg/mL concentrations.⁵⁵

4. CONCLUSIONS

The cosmetic industry has increasingly been focusing on developing products that contain natural bioactive components, such as vitamins, antioxidants, and other nutrients, that can be applied topically to improve the appearance and health of the skin. The present sandalwood oil-based nanoemulsion (NE3) addressed the lacunae of existing cosmetic products by achieving nanosized droplets in the range 50–100 nm. Excellent rheological property and abundance of negative surface potential provide it with longer stability and minimize the flocculation possibilities. The *in vivo* results showed that NE3 has the ability to maintain the structural state of sebaceous glands and increase the levels of palmitic acid and stearic acid in the lipid barrier of burned and rough skin. Additionally, NE3 exhibits greater affinity with key constituents of traditional skincare products, which enables them to minimally induce oxidative stress with a nongenotoxic behavior. In the meantime, our study produced a cutting-edge method for restoring damaged skin that can fulfill the aspirational objectives of the cosmetics industry.

■ AUTHOR INFORMATION

Corresponding Author

Aradhana Mishra – Microbial Technology Division, CSIR-National Botanical Research Institute, Lucknow 226001, India; Academy of Scientific and Innovative Research (AcSIR), Ghaziabad 201002, India; orcid.org/0000-0002-3288-2736; Phone: 91 522 2297987; Email: mishra.a@nbri.res.in, mishramyco@yahoo.com

Authors

Ved Prakash Giri – Microbial Technology Division, CSIR-National Botanical Research Institute, Lucknow 226001, India

Shipra Pandey – Microbial Technology Division, CSIR-National Botanical Research Institute, Lucknow 226001, India; Academy of Scientific and Innovative Research (AcSIR), Ghaziabad 201002, India

Pallavi Shukla – Microbial Technology Division, CSIR-National Botanical Research Institute, Lucknow 226001, India; Academy of Scientific and Innovative Research (AcSIR), Ghaziabad 201002, India

Sateesh Chandra Gupta – Pharmacology Division, CSIR-National Botanical Research Institute, Lucknow 226001, India; Academy of Scientific and Innovative Research (AcSIR), Ghaziabad 201002, India

Manjoosha Srivastava – Phytochemistry Division, CSIR-National Botanical Research Institute, Lucknow 226001, India; Academy of Scientific and Innovative Research (AcSIR), Ghaziabad 201002, India

Chandana Venkateswara Rao – Pharmacology Division, CSIR-National Botanical Research Institute, Lucknow 226001, India; Academy of Scientific and Innovative Research (AcSIR), Ghaziabad 201002, India

Shakti Vinay Shukla – Fragrance & Flavour Development Centre, Kannauj 209726, India

Ashish Dwivedi – Photobiology Division, CSIR-Indian Institute of Toxicology Research, Lucknow 226001, India

Complete contact information is available at:

<https://pubs.acs.org/10.1021/acsomega.3c03811>

Author Contributions

V.P.G.: data curation, formal analysis, methodology, writing-original draft, review, and editing. S.P. and P.S.: data curation, methodology, writing-original draft, review, and editing. S.C.G.: data curation and methodology. M.S. provided facility for rheological analysis. C.V.R. provided animal house facility. S.V.S.: review and editing. A.D. designed experiment for cell line study and provided facility. A.M.: conceptualization, experimental plan, funding acquisition, investigation, supervision, review, and editing. The published version of the manuscript has been read and approved by all authors.

Notes

The authors declare no competing financial interest.

■ ACKNOWLEDGMENTS

The authors would like to thank the Director, CSIR-National Botanical Research Institute, Lucknow, India for providing the necessary facilities to carry out the study. The authors extended thanks to Dr. Alok Lehri for providing the Central Instrumentation Facility (CIF) for the GC-MS analysis. This work is financially supported by the Council of Scientific and Industrial Research (CSIR)-funded project OLP106. Graphical abstract partially created with 'BioRender.com'. The patent application for this work has been approved by India's Intellectual Property (IP) office (Patent No. 0142NF2019/IN). This manuscript has been approved by the institutional ethical committee (MS no. CSIR-NBRI_MS/2023/04/11).

■ REFERENCES

- (1) Marcia, R.-S.; de-Moura-Castro Jacques, C. Epidermal Barrier Function and Systemic Diseases. *Clin. Dermatol.* **2012**, *30* (3), 277–279.
- (2) Egawa, M.; Iwanaga, S.; Hosoi, J.; Goto, M.; Yamanishi, H.; Miyai, M.; Katagiri, C.; Tokunaga, K.; Asai, T.; Ozeki, Y. Label-Free Stimulated Raman Scattering Microscopy Visualizes Changes in

- Intracellular Morphology during Human Epidermal Keratinocyte Differentiation. *Sci. Rep.* **2019**, *9* (1), 1.
- (3) Feingold, K. R.; Elias, P. M. Role of Lipids in the Formation and Maintenance of the Cutaneous Permeability Barrier. *Biochim. Biophys. Acta - Mol. Cell Biol. Lipids* **2014**, *1841* (3), 280–294.
- (4) Kendall, A. C.; Kiezel-Tsugunova, M.; Brownbridge, L. C.; Harwood, J. L.; Nicolaou, A. Lipid Functions in Skin: Differential Effects of N-3 Polyunsaturated Fatty Acids on Cutaneous Ceramides, in a Human Skin Organ Culture Model. *Biochim. Biophys. Acta - Biomembr.* **2017**, *1859* (9), 1679–1689.
- (5) Dayan, N. Stratum Corneum: The Role of Lipids and Ceramides. *Cosmet. Toilet.* **2006**, 37–42.
- (6) Orchard, A.; van Vuuren, S. Commercial Essential Oils as Potential Antimicrobials to Treat Skin Diseases. *Evidence-Based Complement. Altern. Med.* **2017**, *2017*, No. 4517971, DOI: 10.1155/2017/4517971.
- (7) Wertz, P. W. Lipids and Barrier Function of the Skin. *Acta Derm. Venereol.* **2000**, *208*, 7–11.
- (8) Feingold, K. R. Thematic Review Series: Skin Lipids. The Role of Epidermal Lipids in Cutaneous Permeability Barrier Homeostasis. *J. Lipid Res.* **2007**, *48* (12), 2531–2546.
- (9) Silva, J. R.; Burger, B.; Kühl, C. M. C.; Candreva, T.; dos Anjos, M. B. P.; Rodrigues, H. G. Wound Healing and Omega-6 Fatty Acids: From Inflammation to Repair. *Mediat. Inflamm.* **2018**, *2018*, No. 2503950.
- (10) Kang, S. Y.; Um, J. Y.; Chung, B. Y.; Lee, S. Y.; Park, J. S.; Kim, J. C.; Park, C. W.; Kim, H. O. Moisturizer in Patients with Inflammatory Skin Diseases. *Medicina* **2022**, *58* (7), No. 070888.
- (11) Lim, S. H.; Kim, E. J.; Lee, C. H.; Park, G. H.; Yoo, K. M.; Nam, S. J.; Shin, K. O.; Park, K.; Choi, E. H. A Lipid Mixture Enriched by Ceramide NP with Fatty Acids of Diverse Chain Lengths Contributes to Restore the Skin Barrier Function Impaired by Topical Corticosteroid. *Skin Pharmacol. Physiol.* **2022**, *35* (2), 112–123.
- (12) Lin, T. K.; Zhong, L.; Santiago, J. L. Anti-Inflammatory and Skin Barrier Repair Effects of Topical Application of Some Plant Oils. *Int. J. Mol. Sci.* **2018**, *19* (1), 70.
- (13) Sumit, K.; Vivek, S.; Sujata, S.; Ashish, B. Herbal Cosmetics: Used for Skin and Hair. *Inven. J.* **2012**, *2012* (4), 1–7.
- (14) Akter Happy, A.; Jahan, F.; Abdul Momen, M. Essential Oils: Magical Ingredients for Skin Care. *J. Plant Sci.* **2021**, *9* (2), 54.
- (15) Choudhary, S.; Chaudhary, G. Sandalwood (*Santalum Album*): Ancient Tree With Significant Medicinal Benefits. *Int. J. Ayurveda Pharma Res.* **2021**, 90–99.
- (16) Kaul, S.; Gulati, N.; Verma, D.; Mukherjee, S.; Nagaich, U. Role of Nanotechnology in Cosmeceuticals: A Review of Recent Advances. *J. Pharm.* **2018**, *2018*, 1–19.
- (17) Pereira, L. Seaweeds as Source of Bioactive Substances and Skin Care Therapy-Cosmeceuticals, Algoteraphy, and Thalassotherapy. *Cosmetics* **2018**, *5* (4), 68.
- (18) Fanian, F.; Mac-Mary, S.; Jeudy, A.; Lihoreau, T.; Messikh, R.; Ortonne, J. P.; Sainthillier, J. M.; Elkhyat, A.; Guichard, A.; Hejazi Kenari, K.; Humbert, P. Efficacy of Micronutrient Supplementation on Skin Aging and Seasonal Variation: A Randomized, Placebo-Controlled. *Double-Blind Study. Clin. Interv. Aging* **2013**, *8*, 1527–1537.
- (19) Bizot, V.; Cestone, E.; Michelotti, A.; Nobile, V. Improving Skin Hydration and Age-Related Symptoms by Oral Administration of Wheat Glucosylceramides and Digalactosyl Diglycerides: A Human Clinical Study. *Cosmetics* **2017**, *4* (4), 37.
- (20) El-Naggar, M. E.; Abdelgawad, A. M.; Abdel-Sattar, R.; Gibril, A. A.; Hemdan, B. A. Potential Antimicrobial and Antibiofilm Efficacy of Essential Oil Nanoemulsion Loaded polycaprolactone Nanofibrous Dermal Patches. *Eur. Polym. J.* **2023**, *184*, No. 111782.
- (21) Gago, C. M. L.; Artiga-Artigas, M.; Antunes, M. D. C.; Faleiro, M. L.; Miguel, M. G.; Martín-Belloso, O. Effectiveness of Nanoemulsions of Clove and Lemongrass Essential Oils and Their Major Components against *Escherichia Coli* and *Botrytis Cinerea*. *J. Food Sci. Technol.* **2019**, *56* (5), 2721–2736.
- (22) Kowalska, M.; Ziomek, M.; Zbikowska, A. Stability of Cosmetic Emulsion Containing Different Amount of Hemp Oil. *Int. J. Cosmet. Sci.* **2015**, *37* (4), 408–416.
- (23) Pandey, S.; Giri, V. P.; Kumari, M.; Tripathi, A.; Gupta, S. C.; Mishra, A. Comparative Study of the Development and Characterization of Ecofriendly Oil and Water Nanoemulsions for Improving Antifungal Activity. *ACS Agric. Sci. Technol.* **2021**, *1* (6), 640–654.
- (24) Giri, V. P.; Pandey, S.; Kumari, M.; Paswan, S. K.; Tripathi, A.; Srivastava, M.; Rao, C. V.; Katiyar, R.; Nautiyal, C. S.; Mishra, A. Biogenic Silver Nanoparticles as a More Efficient Contraceptive for Wound Healing Acceleration than Common Antiseptic Medicine. *FEMS Microbiol. Lett.* **2019**, *366* (16), No. fnz201.
- (25) Cai, E. Z.; Ang, C. H.; Raju, A.; Tan, K. B.; Hing, E. C. H.; Loo, Y.; Wong, Y. C.; Lee, H.; Lim, J.; Moochhala, S. M.; Hauser, C. A.; Lim, T. C. Creation of Consistent Burn Wounds: A Rat Model. *Arch. Plast. Surg.* **2014**, *41* (4), 317–324.
- (26) Guide for the Care and Use of Laboratory Animals.. *Choice Rev. Online* **1997**, *34* (6), 34-3310. .
- (27) Wang, P.; Sun, M.; Ren, J.; Djuric, Z.; Fisher, G. J.; Wang, X.; Li, Y. Gas Chromatography-Mass Spectrometry Analysis of Effects of Dietary Fish Oil on Total Fatty Acid Composition in Mouse Skin. *Sci. Rep.* **2017**, *7*, 1.
- (28) Bhatia, A.; Bharti, S. K.; Tewari, S. K.; Sidhu, O. P.; Roy, R. Metabolic Profiling for Studying Chemotype Variations in *Withania Somnifera* (L.) Dunal Fruits Using GC-MS and NMR Spectroscopy. *Phytochemistry* **2013**, *93*, 105–115.
- (29) Maurya, V. K.; Sangappa, C.; Kumar, V.; Mahfooz, S.; Singh, A.; Rajender, S.; Jha, R. K. Expression and Activity of Rac1 Is Negatively Affected in the Dehydroepiandrosterone Induced Polycystic Ovary of Mouse. *J. Ovarian Res.* **2014**, *7* (1), 32.
- (30) Suzuki, Y.; Imada, T.; Yamaguchi, I.; Yoshitake, H.; Sanada, H.; Kashiwagi, T.; Takaba, K. Effects of Prolonged Water Washing of Tissue Samples Fixed in Formalin on Histological Staining. *Biotechnol. Histochem.* **2012**, *87* (4), 241–248.
- (31) Dubey, D.; Srivastav, A. K.; Singh, J.; Chopra, D.; Qureshi, S.; Kushwaha, H. N.; Singh, N.; Ray, R. S. Photoexcited Triclosan Induced DNA Damage and Oxidative Stress via p38 MAP Kinase Signaling Involving Type I Radicals under sunlight/UVB Exposure. *Ecotoxicol. Environ. Saf.* **2019**, *174*, 270–282.
- (32) Chopra, D.; Ray, L.; Dwivedi, A.; Tiwari, S. K.; Singh, J.; Singh, K. P.; Kushwaha, H. N.; Jahan, S.; Pandey, A.; Gupta, S. K.; Chaturvedi, R. K.; Pant, A. B.; Ray, R. S.; Gupta, K. C. Photoprotective Efficiency of PLGA-Curcumin Nanoparticles versus Curcumin through the Involvement of ERK/AKT Pathway under Ambient UV-R Exposure in HaCaT Cell Line. *Biomaterials* **2016**, *84*, 25–41.
- (33) Lambers, H.; Piessens, S.; Bloem, A.; Pronk, H.; Finkel, P. Natural Skin Surface pH Is on Average below 5, Which Is Beneficial for Its Resident Flora. *Int. J. Cosmet. Sci.* **2006**, *28* (5), 359–370.
- (34) Ono, S.; Imai, R.; Ida, Y.; Shibata, D.; Komiya, T.; Matsumura, H. Increased Wound pH as an Indicator of Local Wound Infection in Second Degree Burns. *Burns* **2015**, *41* (4), 820–824, DOI: 10.1016/j.burns.2014.10.023.
- (35) Miastkowska, M.; Kulawik-Pióro, A.; Szcurek, M. Nanoemulsion Gel Formulation Optimization for Burn Wounds: Analysis of Rheological and Sensory Properties. *Processes* **2020**, *8* (11), 1416.
- (36) De Azevedo Ribeiro, R. C.; Barreto, S. M. A. G.; Ostrosky, E. A.; Da Rocha-Filho, P. A.; Veríssimo, L. M.; Ferrari, M. Production and Characterization of Cosmetic Nanoemulsions Containing *Opuntia Ficus-Indica* (L.) Mill Extract as Moisturizing Agent. *Molecules* **2015**, *20* (2), 2492–2509.
- (37) Shah, K.; Chan, L. W.; Wong, T. W. Critical Physicochemical and Biological Attributes of Nanoemulsions for Pulmonary Delivery of Rifampicin by Nebulization Technique in Tuberculosis Treatment. *Drug Delivery* **2017**, *24* (1), 1631–1647.
- (38) Safian, M. T. U.; Sekeri, S. H.; Yaqoob, A. A.; Serrà, A.; Jamudin, M. D.; Mohamad Ibrahim, M. N. Utilization of Lignocellulosic Biomass: A Practical Journey towards the Development of Emulsifying Agent. *Talanta* **2022**, *239*, No. 123109.

- (39) Shpichka, A.; Butnaru, D.; Bezrukov, E. A.; Sukhanov, R. B.; Atala, A.; Burdukovskii, V.; Zhang, Y.; Timashev, P. Skin Tissue Regeneration for Burn Injury. *Stem Cell Res. Ther.* **2019**, *10* (1), 1.
- (40) Biswas, R.; Mukherjee, P. K.; Kar, A.; Bahadur, S.; Harwansh, R. K.; Biswas, S.; Al-Dhabi, N. A.; Durairandiyan, V. Evaluation of Ubtan – A Traditional Indian Skin Care Formulation. *J. Ethnopharmacol.* **2016**, *192*, 283–291.
- (41) Moy, R. L.; Levenson, C. Sandalwood Album Oil as a Botanical Therapeutic in Dermatology. *J. Clin. Aesthet. Dermatol.* **2017**, *10* (10), 34–39.
- (42) Anand, U.; Tudu, C. K.; Nandy, S.; Sunita, K.; Tripathi, V.; Loake, G. J.; Dey, A.; Proćków, J. Ethnodermatological Use of Medicinal Plants in India: From Ayurvedic Formulations to Clinical Perspectives – A Review. *J. Ethnopharmacol.* **2022**, *284*, No. 114744.
- (43) Eun Ju, K.; Min-Kyoung, K.; Xing-Ji, J.; Jang-Hee, O.; Ji Eun, K.; Jin Ho, C. Skin Aging and Photoaging Alter Fatty Acids Composition, Including 11,14,17-Eicosatrienoic Acid, in the Epidermis of Human Skin. *J. Korean Med. Sci.* **2010**, *25* (6), 980–983.
- (44) Angerhofer, C. K.; Maes, D.; Giacomoni, P. U. The Use of Natural Compounds and Botanicals in the Development of Anti-Aging Skin Care Products. *Ski. Aging Handb. An Integr. Approach to Biochem. Prod. Dev.* **2009**, 205–263.
- (45) Arda, O.; Göksüğü, N.; Tüzün, Y. Basic Histological Structure and Functions of Facial Skin. *Clin. Dermatol.* **2014**, *32* (1), 3–13.
- (46) Boer, M.; Duchnik, E.; Maleszka, R.; Marchlewicz, M. Structural and Biophysical Characteristics of Human Skin in Maintaining Proper Epidermal Barrier Function. *Postep. Dermatol. Alergol.* **2016**, *33* (1), 1–5.
- (47) Zaid, N. A. M.; Sekar, M.; Bonam, S. R.; Gan, S. H.; Lum, P. T.; Begum, M. Y.; Rani, N. N. I. M.; Vaijanathappa, J.; Wu, Y. S.; Subramaniyan, V.; Fuloria, N. K.; Fuloria, S. Promising Natural Products in New Drug Design, Development, and Therapy for Skin Disorders: An Overview of Scientific Evidence and Understanding Their Mechanism of Action. *Drug Des. Devel. Ther.* **2022**, *16*, 23–66.
- (48) Ghosh, M.; Singh, D.; Singh, A. Recent Advancements in Nanocarrier Based Therapy against Acne: The Role of Biosurfactants and Status of Patents. *Heal. Sci. Rev.* **2023**, *7*, No. 100088.
- (49) Lohani, A.; Verma, A.; Joshi, H.; Yadav, N.; Karki, N. Nanotechnology-Based Cosmeceuticals. *ISRN Dermatol.* **2014**, *2014*, 1–14.
- (50) Patzelt, A.; Lademann, J. Recent Advances in Follicular Drug Delivery of Nanoparticles. *Expert Opin. Drug Delivery* **2020**, *17* (1), 49–60.
- (51) Rai, V. K.; Mishra, N.; Yadav, K. S.; Yadav, N. P. Nanoemulsion as Pharmaceutical Carrier for Dermal and Transdermal Drug Delivery: Formulation Development, Stability Issues, Basic Considerations and Applications. *J. Controlled Release* **2018**, *270*, 203–225.
- (52) Zhou, H.; Luo, D.; Chen, D.; Tan, X.; Bai, X.; Liu, Z.; Yang, X.; Liu, W. Current Advances of Nanocarrier Technology-Based Active Cosmetic Ingredients for Beauty Applications. *Clin. Cosmet. Investig. Dermatol.* **2021**, *14*, 867–887.
- (53) Shukla, S.; Chopra, D.; Patel, S. K.; Negi, S.; Srivastav, A. K.; Ch, R.; Bala, L.; Dwivedi, A.; Ray, R. S. Superoxide Anion Radical Induced Phototoxicity of 2,4,5,6-Tetraminopyrimidine Sulfate via Mitochondrial-Mediated Apoptosis in Human Skin Keratinocytes at Ambient UVR Exposure. *Food Chem. Toxicol.* **2022**, *164*, No. 112990.
- (54) Pacheco, M. T.; Silva, A. C. G.; Nascimento, T. L.; Diniz, D. G. A.; Valadares, M. C.; Lima, E. M. Protective Effect of Sucupira Oil Nanoemulsion against Oxidative Stress in UVA-Irradiated HaCaT Cells. *J. Pharm. Pharmacol.* **2019**, *71* (10), 1532–1543.
- (55) Jerobin, J.; Makwana, P.; Suresh Kumar, R. S.; Sundaramoorthy, R.; Mukherjee, A.; Chandrasekaran, N. Antibacterial Activity of Neem Nanoemulsion and Its Toxicity Assessment on Human Lymphocytes in Vitro. *Int. J. Nanomedicine* **2015**, *10*, 77–86.